Published in final edited form as:
J Biol Chem. 2007 November 2; 282(44): 32520–32528. doi:10.1074/jbc.M707041200.

The Slingshot Family of Phosphatases Mediates Rac1 Regulation of Cofilin Phosphorylation, Laminin-332 Organization, and Motility Behavior of Keratinocytes[*,s]

Kristina Kligys[‡], **Jessica N. Claiborne**[‡], **Phillip J. DeBiase**[‡], **Susan B. Hopkinson**[‡], **Yvonne Wu**[‡], **Kensaku Mizuno**[§], and **Jonathan C. R. Jones**[‡,1]

[‡] Department of Cell and Molecular Biology, Feinberg School of Medicine, Northwestern University, Chicago, Illinois 60611

[§] Department of Biomolecular Sciences, Graduate School of Life Sciences, Tohoku University, Sendai, Miyagi 980-8578, Japan

Abstract

The motility of keratinocytes is an essential component of wound closure and the development of epidermal tumors. *In vitro*, the specific motile behavior of keratinocytes is dictated by the assembly of laminin-332 tracks, a process that is dependent upon $\alpha6\beta4$ integrin signaling to Rac1 and the actin-severing protein cofilin. Here we have analyzed how cofilin phosphorylation is regulated by phosphatases (slingshot (SSH) or chronophin (CIN)) downstream of signaling by $\alpha6\beta4$ integrin/Rac1 in human keratinocytes. Keratinocytes express all members of the SSH family (SSH1, SSH2, and SSH3) and CIN. However, expression of phosphatase-dead versions of all three SSH proteins, but not dominant inactive CIN, results in phosphorylation/inactivation of cofilin, changes in actin cytoskeleton organization, loss of cell polarity, and assembly of aberrant arrays of laminin-332 in human keratinocytes. SSH activity is regulated by 14-3-3 protein binding, and intriguingly, 14-3-3/$\alpha6\beta4$ integrin protein interaction is required for keratinocyte migration. We wondered whether 14-3-3 proteins function as regulators of Rac1-mediated keratinocyte migration patterns. In support of this hypothesis, inhibition of Rac1 results in an increase in 14-3-3 protein association with SSH. Thus, we propose a novel mechanism in which $\alpha6\beta4$ integrin signaling via Rac1, 14-3-3 proteins, and SSH family members regulates cofilin activation, cell polarity, and matrix assembly, leading to specific epidermal cell migration behavior.

The role $\alpha6\beta4$ integrin plays in the adhesion of cells to the extracellular matrix has been well elucidated (1,2). In an intact epithelium, $\alpha6\beta4$ integrin functions as a cell surface receptor for laminin-332 (laminin-5) and as a scaffold for the formation of matrix-adhesive structures termed hemidesmosomes (3–6). Indeed, expression of the $\alpha6\beta4$ integrin is critical for maintaining epidermal cell integrity with the basement membrane, because mice lacking $\beta4$ integrin exhibit extensive skin blisters and the loss of $\beta4$ integrin expression in humans is a cause of the blistering skin disease junctional epidermolysis bullosa (4,7–9). The latter data have led to the notion that the primary function of $\alpha6\beta4$ integrin is to mediate stable anchorage of cells to matrix, a property that would antagonize cell migration (1,3,5). However, a number

[*]This work was supported by National Institutes of Health Grant R01 AR054184 (to J. C. R. J.) and National Institutes of Health Training Grant T32 HL076139 (to K. K.).

[s]The on-line version of this article (available at http://www.jbc.org) contains supplemental Figs. S1 and S2 and supplemental Videos S1–S3.

1To whom correspondence should be addressed: Dept. of Cell and Molecular Biology, Feinberg School of Medicine, Northwestern University, 303 E. Chicago Ave., Chicago, IL 60611. Tel.: 312-503-1412; Fax: 312-503-6475; E-mail: j-jones3@northwestern.edu.

of studies have shown that during wound healing and metastasis, $\alpha 6\beta 4$ integrin is also an important mediator of cell migration and the invasion of tumor cells (10–15). Under these circumstances, $\alpha 6\beta 4$ integrin modulates both the activity and signaling of phosphatidylinositol 3-kinase and/or the small GTPase Rac1 leading to cell migration (11,14,16–18).

Rac1, together with other Rho family proteins, Rho and Cdc42, can be activated by integrins in a variety of cell types and mediates signaling cascades that ultimately promote cell motility (19–21). We recently showed that Rac1, via the actin-severing protein cofilin, regulates the migration of keratinocytes by determining the precise supramolecular organization of laminin-332 in their extracellular matrices. Specifically, in keratinocytes, expression of a dominant negative Rac1 or treatment with a Rac1 chemical inhibitor results in phosphorylation of cofilin at serine residue 3 (14,22–24). Phosphorylated cofilin is either inactive or possibly mislocalized in such keratinocytes, leading to aberrant cell migration over circles of laminin-332 matrix (14,25,26). In other words, dephosphorylation of cofilin is a necessary prerequisite for “proper” keratinocyte motility behavior along an appropriately arrayed matrix track of laminin-332 *in vitro* (14). In a tissue context of wound healing or metastasis, this is an important phenomenon because tracks of laminin-332 likely play a key role in regulating directed migration of keratinocytes over connective tissue during coverage of wounds or through the extracellular matrix during invasion (27–33).

In this study, we have investigated the molecular mechanisms by which Rac1 activity leads to dephosphorylation of cofilin and the specification of migration behavior in keratinocytes. Previous data in neuronal cells have suggested that Rac1 activity leads to cofilin dephosphorylation through the positive regulation of LIM kinase (23,25). Conversely, we have shown previously that Rac1 activation leads to a dephosphorylation of cofilin in human epidermal cells (11,14,16–18). In this regard, two distinct families of phosphatases have been shown to dephosphorylate cofilin at serine residue 3. These include the slingshot (SSH)[2] family of phosphatases and the haloacid dehalogenase phosphatase, chronophin (CIN) (34–36). In this study we have uncovered a novel pathway by which $\alpha 6\beta 4$ integrin/Rac1 signals to SSH family members, thereby resulting in modulation of cell migration patterns of keratinocytes.

EXPERIMENTAL PROCEDURES

Reagents, Cell Culture, and Antibodies

Human epidermal keratinocytes, immortalized with human papilloma virus genes E6 and E7, were described previously (14). The cells were maintained in defined keratinocyte serum-free medium supplemented with a 1% penicillin/streptomycin/neomycin mixture (Invitrogen Corp.) and grown at 37 °C. The Rac1 inhibitor NSC23766 was obtained from Calbiochem and added to growth medium at a concentration of 50 μM. Rabbit polyclonal antibodies against Ser-3-phosphorylated cofilin and total cofilin were purchased from Cell Signaling Technology (Beverly, MA). Rabbit monoclonal antibody against β-actin was obtained from Epitomics, Inc. (Burlingame, CA). Mouse monoclonal antibody against the V5 epitope tag was purchased from Invitrogen. 9E10, a mouse monoclonal antibody against the c-Myc epitope, was derived from the supernatant of a hybridoma line purchased from the American Type Culture Collection (Rockville, MD). Rabbit pan-14-3-3 antibody was purchased from Santa Cruz Biotechnology, Inc. (Santa Cruz, CA). Mouse monoclonal antibody against green fluorescent protein was purchased from Roche Applied Science. The rabbit polyclonal antibody against SSH1 was described previously (37). Rabbit polyclonal antibodies against SSH2 or SSH3 were raised against the peptides ANDKKRTT-NPFYNTM and CFRKVVRQASVHDSGEEGEA, respectively. Rabbit polyclonal antibody against CIN was purchased from Cell Signaling

[2]The abbreviations used are: SSH, slingshot; CIN, chronophin; CIN D/N, dominant inactive CIN.

Technology. The mouse monoclonal antibody against the γ2 chain of laminin-332 (GB3) was purchased from Harlan Sera-Lab Ltd. (England). Rhodamine phalloidin was obtained from Invitrogen.

Adenoviral Constructs

Plasmids encoding the human wild type SSH2 protein or phosphatase-dead SSH proteins (SSH1CS, SSH2CS, and SSH3CS) were described previously (34,36,37). cDNA encoding each of these SSH proteins was subcloned into the polylinker of the pENTR4 vector (Invitrogen). The SSH1CS and SSH3CS/pENTR clones were used in a site-directed recombination reaction to place these cDNAs into the pAD/CMV/V5-DEST vector (Invitrogen) in-frame with sequences encoding the V5 tag, according to the manufacturer's protocol. The wild type SSH2 and SSH2CS cDNAs each contained an in-frame c-Myc tag, and these fusion constructs were placed into the pAD/CMV/V5-DEST. The plasmid encoding dominant inactive CIN (CIN D/N) was kindly provided by Dr. Gary Bokoch (Scripps Research Institute, La Jolla, CA). The CIN D/N cDNA was subcloned into the polylinker of pENTR4 and subsequently placed into the pAD/CMV/V5-DEST. Each of the adenoviral expression clones was introduced into 293A cells by Lipofectamine-mediated transfection. After 10–12 days, the crude viral lysate was harvested and used to amplify the adenovirus as previously described (14). The amplified viral stock was titered, and epithelial cells were infected at a multiplicity of infection of 1:50 in cell medium.

Cell Motility

Scratch assays on confluent monolayers of wild type cells and cells infected with SSH1CS, SSH2CS, SSH3CS, CIN D/N, or control adenovirus were performed as described previously (38). Single cell motility was measured as detailed by Sehgal *et al*. (14). Briefly, cells were plated onto uncoated 35-mm glass-bottomed culture dishes (MatTek Corp., Ashland, MA) 18–24 h prior to cell motility assays. Cells were viewed on a Nikon TE2000 inverted microscope (Nikon Inc., Melville, NY). Images were taken at 2-min intervals over 2 h, and cell motility behavior was analyzed by a MetaMorph Imaging System (Universal Imaging Corp., Molecular Devices, Downingtown, PA). Motility assays were performed a minimum of three times. For migration on preformed matrices, keratinocytes were allowed to adhere to uncoated 35-mm glass-bottomed culture dishes overnight. The cells were rinsed with phosphate-buffered saline and treated with 20 mM NH_4OH for 5 min to remove cells, leaving the laminin-332-rich matrix behind (11,14,16–18). The plates were washed extensively with water and rinsed with phosphate-buffered saline. Keratinocytes infected with various adenoviruses were plated directly onto the isolated matrix, allowed to adhere for 2–4 h, and imaged over an additional period of 2 h as described above.

Fluorescence Microscopy

Cells plated onto glass coverslips were processed for microscopical analyses as detailed elsewhere (39). All preparations were viewed with a Zeiss laser-scanning 510 confocal microscope (Zeiss Inc., Thornwood, NY). Images were exported as TIFF files, and figures were generated using Adobe Photoshop software.

SDS-PAGE, Immunoblotting, and Immunoprecipitation

Whole cell extracts from ~0.5×10^6 cells were prepared by solubilization in 1% SDS, 8 M urea, 10% glycerol, 5% β-mercaptoethanol, 25 mM Tris-HCl, pH 6.5. The proteins were separated by SDS-PAGE, transferred to nitrocellulose, and processed for immunoblotting as previously described (14,39). For immunoprecipitation analyses, cells treated with or without Rac1 inhibitor were extracted in 20 mM Tris-HCl, pH 7.5, 150 mM NaCl, 5 mM EDTA, 1% Triton X-100, 20 mM β-glycerophosphate, 10% glycerol, 0.5 mM dithiothreitol, 20 mM NaF,

1 mM $NaOV_3$ supplemented with the protease inhibitors phenylmethylsulfonyl fluoride and leupeptin. Cell lysates were centrifuged for 10 min at 12,000 × *g*. One-tenth of the lysate was saved as a loading control in immunoblotting studies. For immunoprecipitation of SSH1 and SSH3, anti-V5-conjugated agarose beads (Sigma-Aldrich) were added to the lysate and incubated for 1.5 h at 4 °C on a rocking platform. Immunoprecipitation of SSH2 was performed as described above, except with anti-Myc-conjugated beads (Sigma-Aldrich). The beads were washed with phosphate-buffered saline and collected by centrifugation. Following the last wash, a sample buffer (6% SDS, 10% glycerol, 5% *β*-mercaptoethanol, 25 mM Tris-HCl, pH 6.5) was added to the bead pellet. The sample was boiled for 10 min, processed for SDS-PAGE, transferred to nitrocellulose, and processed for immunoblotting as above. Immunoblots were scanned and quantified using a MetaMorph Imaging System.

RESULTS

SSH Proteins Are Expressed in Keratinocytes and Regulate Cofilin Phosphorylation

The SSH family of phosphatases and the phosphatase CIN are known to regulate cofilin activity (34–36,40). To assess whether the SSHs and/or CIN protein might regulate the phosphorylation state of cofilin in human keratinocytes, we first assayed whether these proteins are expressed in epidermal cells. Fig. 1 shows Western blot analyses of an extract of human keratinocytes probed with antibodies specific for each of the three members of the SSH family (SSH1, SSH2, and SSH3) and CIN. Human keratinocytes express all three SSH family members (Fig. 1, *lanes 1–3*). CIN expression is also seen in these cells (*lane 4*). We next investigated which of these proteins regulates cofilin activity using a molecular genetic approach. Human keratinocytes were infected with adenovirus encoding phosphatase-dead (CS) SSH family members (SSH1CS, SSH2CS, and SSH3CS) or adenovirus encoding dominant inactive CIN (CIN D/N). Expression of the phosphatase-dead SSH proteins has been shown to inhibit endogenous SSH phosphatase activity (34,36,37). The SSH1CS and SSH3CS proteins were tagged with the V5 epitope while SSH2CS was tagged with the c-Myc epitope. Western blotting was used to confirm expression of each of the phosphatase-dead mutants as well as the dominant inactive CIN in the infected keratinocytes (Fig. 2*A*). At 48 h after infection of each of our cell populations, we assayed the phosphorylation level of cofilin. Expression of the CIN D/N protein had no effect on the levels of phosphorylated cofilin when compared with controls (Fig. 2*B*). In sharp contrast, phosphocofilin levels in keratinocytes overexpressing SSH1CS, SSH2CS, or SSH3CS were increased more than 2-fold over that observed in control cells (Fig. 2*B*). Taken together, these results suggest that the SSH family of phosphatases and not the phosphatase CIN regulates cofilin phosphorylation in human epidermal cells.

Cofilin Inactivation by Phosphatase-dead SSH Proteins Modulates the Actin Cytoskeleton and Polarity of Human Keratinocytes

We previously presented evidence that *α*6*β*4 integrin signaling to cofilin regulates motility behavior (14). Because SSH proteins have been shown to bind F-actin and affect actin depolymerization by dephosphorylating cofilin (34,41), we next asked whether expression of dominant negative SSH proteins might impact actin cytoskeleton organization in keratinocytes. Cells infected with adenovirus encoding SSH1CS, SSH2CS, SSH3CS, or CIN D/N were plated at subconfluency on uncoated surfaces and 48 h later were fixed and stained with rhodamine-phalloidin. The images in Fig. 3, *left panels*, depict select examples of staining patterns observed. These patterns were quantified (*right panels*). Uninfected keratinocytes, control-infected keratinocytes, and cells expressing CIN D/N are highly polarized, often exhibiting a single fan-shaped lamellipodia at the leading edge of the cell and retraction fibers at the cell rear (Fig. 3, *left panels*; only uninfected keratinocytes and keratinocytes expressing CIN D/N are shown). Within the control and CIN D/N-expressing cells, F-actin is organized into fibrillar arcs toward the leading edge of the polarized cells and is also localized in retraction fibers

(*left panels*). Moreover, the majority of the uninfected keratinocytes, control-infected keratinocytes, and cells expressing CIN D/N exhibit only one lamellipodium per cell (Fig. 3, *right panel graphs*). In sharp contrast, the number of lamellipodia per cell in keratinocytes expressing phosphatase-dead SSH proteins varies from none to three (*right panel graphs*). Furthermore, these cells fail to exhibit any obvious polarity; they do not appear fan-shaped (*left panels*). Specifically, cells expressing phosphatase-dead SSH proteins are either rounded with few, if any, lamellipodia or contain multiple lamellipodia and display a cortical actin ring at the perimeter of the cells (*left panels*).

Phosphatase-dead SSHs, but Not Dominant Inactive CIN, Induce Aberrant Motility of Human Keratinocytes over Circular Arrays of Laminin-332

Published data from our laboratory have demonstrated that wild type keratinocytes move back and forth on defined laminin-332 matrix tracks (14). In contrast, keratinocytes expressing dominant negative Rac1 or dominant inactive cofilin migrate in a circular-like pattern, regulated by circular arrays of laminin-332 in their matrix (14). Based on these precedents we predicted that wild type keratinocytes, induced to express phosphatase-dead SSH proteins leading to an increase in cofilin phosphorylation, should similarly exhibit abnormal motile behavior and assemble an aberrant laminin-332 matrix. To test these predictions, keratinocytes infected with control adenovirus or adenovirus encoding CIN D/N, SSH1CS, SSH2CS, or SSH3CS were plated on glass, and migration of the cells was monitored by phase-contrast microscopy over a 2-h period (Fig. 4). The different cell populations show no significant differences in migration rate or directionality, consistent with our previous report (not shown) (14). However, this was not the case when we analyzed the patterns of their migration by vector diagram (supplemental Fig. S1). We observed two major motility behaviors in each of our cell populations, movement along primarily linear paths/trails and circular migration. These behaviors were quantified (Fig. 4). The majority of uninfected keratinocytes, keratinocytes infected with control virus, and keratinocytes expressing CIN D/N migrate along tracks in a backtracking motion (Fig. 4,supplemental Fig. S1, and supplemental Video S1) (14). In sharp contrast, expression of all three phosphatase-dead SSH proteins induces cells to migrate primarily along circular paths (Fig. 4, supplemental Fig. S1). An example of the motility behavior exhibited by keratinocytes expressing SSH1CS is shown in supplementary Video S2.

Keratinocytes infected with control adenovirus or adenovirus encoding SSH1CS, SSH2CS, SSH3CS, or CIN D/N were also processed for indirect immunofluorescence microscopical analyses using a monoclonal antibody against the γ2 subunit of laminin-332. Three distinct staining patterns of laminin-332 were observed in these cells, a snail-like trail of laminin-332, laminin-332 organized into discrete circles, and laminin-332 deposited directly beneath the cells in a diffuse pattern (Fig. 5). We quantified the laminin-332 patterns in our cell populations (Fig. 5, *right panel graphs*). The images are representative of the staining pattern observed in the majority of the cells. In ~60% of keratinocytes expressing the phosphatase-dead SSH proteins, laminin-332 is deposited onto the substrate in ring-like arrays (*right panel graphs*). Less than 10% of the cells secrete laminin-332 in trails. In contrast, in >40% of uninfected keratinocytes, control-infected keratinocytes, or keratinocytes expressing CIN D/N, laminin-332 is deposited in snail-like trails (Fig. 5). Only ~20% of these cells deposit laminin-332 into ring-like structures on their substrate (Fig. 5). The pattern of laminin-332 organization in the matrix of the cells is reflected in their motility behavior (compare graphs in Figs. 4 and 5).

We next assayed migration of cells in a scratch wound assay. Keratinocytes expressing phosphatase-dead SSH proteins display significantly slower wound closure compared with uninfected or control infected keratinocytes (supplemental Fig. S2).

Together, these results imply that in keratinocytes SSH proteins regulate cofilin activity which, in turn, determines cell polarity and, hence, deposition of patterns of matrix that precisely specify cell motility behavior. Alternatively, SSH proteins might regulate the internal motile machinery of a cell, thereby specifying motility patterns, regardless of matrix organization. To distinguish these possibilities, keratinocytes expressing SSH1CS were plated onto the laminin-332 matrix of wild type keratinocytes. The motility behavior of these cells was then monitored at 4 h after plating onto the preformed matrix (14,28,33). Under these conditions, a majority of the infected cells move in linear trails over the preformed laminin-332-rich substrate and appear polarized, despite the increase in phospho-cofilin levels in the infected cells (Fig. 6, *A–C*, and supplemental Video S3). Similar results were obtained using keratinocytes infected with adenovirus encoding SSH2CS and SSH3CS (not shown). Therefore, our results strongly suggest that the matrix is an important regulator of the specific motility pattern of keratinocytes.

14-3-3 Protein Binding to SSH Proteins in Motile Cells Versus Cells Exhibiting Aberrant Motility Behavior

Our previous report defined cofilin as a determinant of migration and matrix organization in keratinocytes through the activity of $\alpha 6\beta 4$ integrin/Rac1 signaling (14). The above data suggest that SSH is also downstream of $\alpha 6\beta 4$ integrin/Rac1 signaling. To further delineate the molecular mechanisms underpinning the control of keratinoycte migration, we asked how Rac1 signaling activates SSH activity. SSH proteins have been shown to be negatively regulated by phosphorylation of serine residues (42,43). Several 14-3-3 isoforms bind to sequences adjacent to these phosphorylated serine residues and inactivate SSH by inhibiting its phosphatase activity (22,44). This interaction potentially impedes cell motility (22). Interestingly, several 14-3-3 isoforms can also bind to phosphorylated $\alpha 6\beta 4$ integrin (45), but this binding leads to the displacement of $\alpha 6\beta 4$ integrin from hemidesmosomes to lamellipodia and an induction of cell migration (45). Because 14-3-3 binding to SSH or $\alpha 6\beta 4$ integrin differentially regulates their activities, we wondered whether 14-3-3 proteins might be key regulators in the signaling pathway linking $\alpha 6\beta 4$ integrin, through Rac1, to SSH proteins. To test this hypothesis, we assayed 14-3-3 protein/SSH interaction in untreated, subconfluent, motile keratinocytes and similarly in subconfluent keratinocytes that were pretreated with the Rac1 inhibitor NSC23766. Rac1 inhibitor treatment inhibits $\beta 4$ integrin signaling to cofilin, resulting in aberrant motility behavior (14). Because the SSH proteins that we expressed in keratinocytes were tagged with V5 (SSH1 and SSH3) or c-Myc (SSH2) epitopes, we analyzed SSH protein interaction with 14-3-3 proteins using V5- or c-Myc-conjugated agarose beads. There is an ~2-fold increase in 14-3-3 protein/SSH interaction in extracts of keratinocytes treated with Rac1 inhibitor compared with extracts derived from untreated cells (Fig. 7, *A–C*). 14-3-3 binding to SSH proteins is observed with SSH1, SSH2, and SSH3 (*panels A–C*, respectively).

DISCUSSION

Healing of wounded skin is a complex process, a central element of which involves directed motility of keratinocytes over a wound bed. Directed migration of tumor keratinocytes is also fundamental to metastasis and the movement of cancer cells away from the origin of a tumor. Our goal is to define the pathway by which $\beta 4$ integrin regulates the laminin-332 tracks over which keratinocytes migrate (14). We have already reported that $\alpha 6\beta 4$ integrin regulates laminin-332 matrix assembly and, hence, keratinocyte migration behavior by signaling through Rac1 to the actin-severing protein cofilin (14). In our previous study, we showed that Rac1 signaling to cofilin in epithelial cells is distinct from the pathway that has been published for neuronal cells (24). In neuronal cells, Rac1 signals through p-21-activated kinase to phosphorylate/inactivate cofilin (23). However, in keratinocytes, the opposite is the case. $\alpha 6\beta 4$ integrin signaling via Rac1 maintains active cofilin (14). Here, we have extended these

results by showing that members of the SSH phosphatase family are downstream of $\alpha 6\beta 4$ integrin/Rac1 signaling and are responsible for the regulation of cofilin activity in epidermal cells.

The SSH family of phosphatases contains three family members, each of which has the ability to dephosphorylate cofilin (36). Because all three are expressed by keratinocytes, all three may play roles in defining skin cell motility behavior. Indeed, our data indicate that inactivation of each of the different SSH proteins in keratinocytes leads to an aberrant motility phenotype. This suggests that there is no compensation between the different SSH proteins, at least in keratinocytes. However, we cannot rule out the possibility that each of the phosphatase-dead SSH proteins we used in our analyses targets all SSH family members. Nonetheless, our data clearly indicate that SSH proteins are key regulators of lamellipodia formation and motility behavior. This is consistent with work in Jurkat cells in which SSH1 has been knocked down (46). Furthermore, because it is well accepted that Rac activity is involved in the formation of the lamellipodium at the leading edge of the cell (47), we suggest that Rac1 activity mediates migration by regulating local SSH activity.

How is the activity of SSH proteins precisely regulated in keratinocytes? SSH proteins, when phosphorylated on serine residues, bind 14-3-3 proteins, which results in sequestering of SSH proteins into the cytoplasm and their inactivation (22,42). 14-3-3 proteins also have been shown to interact with phosphorylated $\alpha 6\beta 4$ integrin tails when keratinocytes are induced to migrate (45). Thus, we propose that 14-3-3 protein isoforms function either to promote or to inhibit migration of keratinocytes. Experimental evidence in support of this mechanism comes from our immunoprecipitation analyses. Consistent with previous studies (45), we detect a $\beta 4$ integrin/14-3-3 interaction in migrating keratinocytes (data not shown). In contrast, in these motile keratinocytes there is less 14-3-3 protein association with SSH proteins compared with keratinocytes in which motility is impaired.

We have presented evidence that all three SSH family members exhibit interaction with 14-3-3 proteins. To our knowledge, such an interaction has only been described for SSH1 (22,42). In this regard, the SSH1 domain involved in 14-3-3 binding has been shown to be near the serine-rich region at the carboxyl terminus of the molecule (22,42). A homologous domain is present in SSH2, but not SSH3 (36). Thus, SSH3 apparently possesses a 14-3-3 binding domain distinct from that of SSH1.

One intriguing aspect of our study relates to whether the polarity of a cell determines the organization of its extracellular matrix or *vice versa.* Specifically, do $\alpha 6\beta 4$ integrin and Rac1, through control of SSH protein activity, define cell polarity that, in turn, regulates matrix organization and cell motility behavior or do these proteins primarily regulate laminin-332 matrix organization, which dictates cell polarity? Our data would indicate that the latter is the case. Epidermal cells lacking $\beta 4$ integrin or cells in which the activity of SSH proteins Rac1 or cofilin have been inhibited lack polarization and migrate in circles. However, these same cells appear polarized and migrate like their wild type counterparts provided they are maintained on the matrix deposited by wild type epidermal cells (14). In other words, matrix organization is a primary determinant of keratinocyte polarity.

In conclusion, we describe the molecular events by which $\alpha 6\beta 4$ integrin regulates cell motility via its ability to determine laminin-332 organization. Our results underscore the dual role of this molecule as a determinant of stable attachment and as a mediator of matrix assembly. Moreover, our data lead us to propose the following model. In migrating keratinocytes, $\alpha 6\beta 4$ integrin-14-3-3 protein complexes function as a scaffold for Rac1, thereby regulating a downstream signaling cascade (Fig. 8). This cascade activates as-yet unknown phosphatases that promote the maintenance of dephosphorylated SSH proteins. Active SSH proteins

dephosphorylate cofilin, ultimately allowing for local actin depolymerization at the leading edge of the cell, increasing $\alpha 6\beta 4$ integrin dynamics, and a concomitant modeling of laminin-332 matrix to generate a trail over which cells move. On the other hand, in stationary cells (or in cells exhibiting aberrant motility due to a lack of $\beta 4$ integrin), Rac1 activity is low and 14-3-3 protein association with SSH proteins is enhanced, leading to SSH protein sequestration and inhibition (14,28,33). Under these conditions, cofilin is kept in a phosphorylated/inactive state, thus inhibiting the dynamic activity of $\beta 4$ integrin, the organization of laminin-332 into trails, and "proper" keratinocyte motility.

Supplementary Material

Refer to Web version on PubMed Central for supplementary material.

References

1. Litjens SH, de Pereda JM, Sonnenberg A. Trends Cell Biol 2006;16:376–383. [PubMed: 16757171]
2. Borradori L, Sonnenberg A. J Investig Dermatol 1999;112:411–418. [PubMed: 10201522]
3. Jones JC, Hopkinson SB, Goldfinger LE. BioEssays 1998;20:488–494. [PubMed: 9699461]
4. Dowling J, Yu QC, Fuchs E. J Cell Biol 1996;134:559–572. [PubMed: 8707838]
5. Jones JC, Kurpakus MA, Cooper HM, Quaranta V. Cell Regul 1991;2:427–438. [PubMed: 1883873]
6. Aumailley M, Bruckner-Tuderman L, Carter WG, Deutzmann R, Edgar D, Ekblom P, Engel J, Engvall E, Hohenester E, Jones JC, Kleinman HK, Marinkovich MP, Martin GR, Mayer U, Meneguzzi G, Miner JH, Miyazaki K, Patarroyo M, Paulsson M, Quaranta V, Sanes JR, Sasaki T, Sekiguchi K, Sorokin LM, Talts JF, Tryggvason K, Uitto J, Virtanen I, von der Mark K, Wewer UM, Yamada Y, Yurchenco PD. Matrix Biol 2005;24:326–332. [PubMed: 15979864]
7. Jonkman MF. J Dermatol Sci 1999;20:103–121. [PubMed: 10379703]
8. van der Neut R, Krimpenfort P, Calafat J, Niessen CM, Sonnenberg A. Nat Genet 1996;13:366–369. [PubMed: 8673140]
9. Jonkman MF, Pas HH, Nijenhuis M, Kloosterhuis G, Steege G. J Investig Dermatol 2002;119:1275–1281. [PubMed: 12485428]
10. Rabinovitz I, Mercurio AM. J Cell Biol 1997;139:1873–1884. [PubMed: 9412479]
11. Mercurio AM, Rabinovitz I, Shaw LM. Curr Opin Cell Biol 2001;13:541–545. [PubMed: 11544021]
12. Nikolopoulos SN, Blaikie P, Yoshioka T, Guo W, Giancotti FG. Cancer Cell 2004;6:471–483. [PubMed: 15542431]
13. Nikolopoulos SN, Blaikie P, Yoshioka T, Guo W, Puri C, Tacchetti C, Giancotti FG. Mol Cell Biol 2005;25:6090–6102. [PubMed: 15988021]
14. Sehgal BU, DeBiase PJ, Matzno S, Chew TL, Claiborne JN, Hopkinson SB, Russell A, Marinkovich MP, Jones JC. J Biol Chem 2006;281:35487–35498. [PubMed: 16973601]
15. Dajee M, Lazarov M, Zhang JY, Cai T, Green CL, Russell AJ, Marinkovich MP, Tao S, Lin Q, Kubo Y, Khavari PA. Nature 2003;421:639–643. [PubMed: 12571598]
16. Shaw LM, Rabinovitz I, Wang HH, Toker A, Mercurio AM. Cell 1997;91:949–960. [PubMed: 9428518]
17. Giannelli G, Astigiano S, Antonaci S, Morini M, Barbieri O, Noonan DM, Albini A. Clin Exp Metastasis 2002;19:217–223. [PubMed: 12067202]
18. Gilcrease MZ, Zhou X, Welch K. Cancer Res 2004;64:7395–7398. [PubMed: 15492261]
19. Berrier AL, Martinez R, Bokoch GM, LaFlamme SE. J Cell Sci 2002;115:4285–4291. [PubMed: 12376560]
20. Danen EH, van Rheenen J, Franken W, Huveneers S, Sonneveld P, Jalink K, Sonnenberg A. J Cell Biol 2005;169:515–526. [PubMed: 15866889]
21. Fujiwara H, Gu J, Sekiguchi K. Exp Cell Res 2004;292:67–77. [PubMed: 14720507]
22. Nagata-Ohashi K, Ohta Y, Goto K, Chiba S, Mori R, Nishita M, Ohashi K, Kousaka K, Iwamatsu A, Niwa R, Uemura T, Mizuno K. J Cell Biol 2004;165:465–471. [PubMed: 15159416]

23. Edwards DC, Sanders LC, Bokoch GM, Gill GN. Nat Cell Biol 1999;1:253–259. [PubMed: 10559936]
24. Maekawa M, Ishizaki T, Boku S, Watanabe N, Fujita A, Iwamatsu A, Obinata T, Ohashi K, Mizuno K, Narumiya S. Science 1999;285:895–898. [PubMed: 10436159]
25. Yang N, Higuchi O, Ohashi K, Nagata K, Wada A, Kangawa K, Nishida E, Mizuno K. Nature 1998;393:809–812. [PubMed: 9655398]
26. Song X, Chen X, Yamaguchi H, Mouneimne G, Condeelis JS, Eddy RJ. J Cell Sci 2006;119:2871–2881. [PubMed: 16803871]
27. Miyazaki K. Cancer Sci 2006;97:91–98. [PubMed: 16441418]
28. Zhang K, Kramer RH. Exp Cell Res 1996;227:309–322. [PubMed: 8831569]
29. Qin P, Kurpakus MA. Exp Eye Res 1998;66:569–579. [PubMed: 9628804]
30. O'Toole EA. Clin Exp Dermatol 2001;26:525–530. [PubMed: 11678882]
31. Kariya Y, Miyazaki K. Exp Cell Res 2004;297:508–520. [PubMed: 15212952]
32. Hintermann E, Quaranta V. Matrix Biol 2004;23:75–85. [PubMed: 15246107]
33. Frank DE, Carter WG. J Cell Sci 2004;117:1351–1363. [PubMed: 14996912]
34. Niwa R, Nagata-Ohashi K, Takeichi M, Mizuno K, Uemura T. Cell 2002;108:233–246. [PubMed: 11832213]
35. Gohla A, Birkenfeld J, Bokoch GM. Nat Cell Biol 2005;7:21–29. [PubMed: 15580268]
36. Ohta Y, Kousaka K, Nagata-Ohashi K, Ohashi K, Muramoto A, Shima Y, Niwa R, Uemura T, Mizuno K. Genes Cells 2003;8:811–824. [PubMed: 14531860]
37. Kaji N, Ohashi K, Shuin M, Niwa R, Uemura T, Mizuno K. J Biol Chem 2003;278:33450–33455. [PubMed: 12807904]
38. Goldfinger LE, Hopkinson SB, deHart GW, Collawn S, Couchman JR, Jones JC. J Cell Sci 1999;112:2615–2629. [PubMed: 10413670]
39. Tsuruta D, Hopkinson SB, Lane KD, Werner ME, Cryns VL, Jones JC. J Biol Chem 2003;278:38707–38714. [PubMed: 12867433]
40. Endo M, Ohashi K, Sasaki Y, Goshima Y, Niwa R, Uemura T, Mizuno K. J Neurosci 2003;23:2527–2537. [PubMed: 12684437]
41. Yamamoto M, Nagata-Ohashi K, Ohta Y, Ohashi K, Mizuno K. FEBS Lett 2006;580:1789–1794. [PubMed: 16513117]
42. Soosairajah J, Maiti S, Wiggan O, Sarmiere P, Moussi N, Sarcevic B, Sampath R, Bamburg JR, Bernard O. EMBO J 2005;24:473–486. [PubMed: 15660133]
43. Nishita M, Wang Y, Tomizawa C, Suzuki A, Niwa R, Uemura T, Mizuno K. J Biol Chem 2004;279:7193–7198. [PubMed: 14645219]
44. Sarmiere PD, Bamburg JR. J Neurobiol 2004;58:103–117. [PubMed: 14598374]
45. Santoro MM, Gaudino G, Marchisio PC. Dev Cell 2003;5:257–271. [PubMed: 12919677]
46. Nishita M, Tomizawa C, Yamamoto M, Horita Y, Ohashi K, Mizuno K. J Cell Biol 2005;171:349–359. [PubMed: 16230460]
47. Ridley AJ, Paterson HF, Johnston CL, Diekmann D, Hall A. Cell 1992;70:401–410. [PubMed: 1643658]

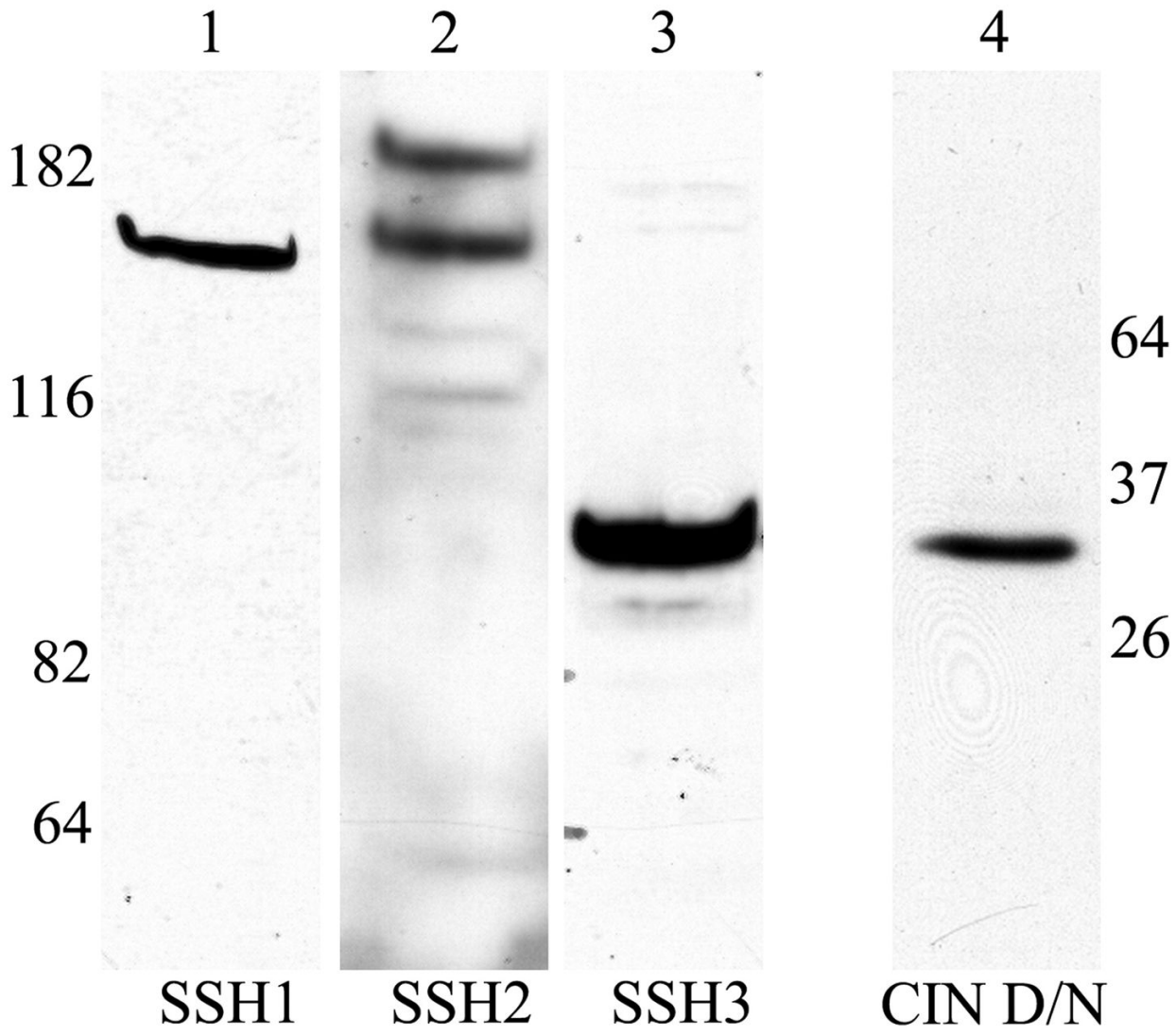

FIGURE 1. Expression of SSH and CIN proteins in human keratinocytes

Whole cell extracts of keratinocytes were processed for Western immunoblotting using antibodies against SSH1 (*lane 1*), SSH2 (*lane 2*), SSH3 (*lane 3*), or CIN (*lane 4*). Samples in *lanes 1–3* were processed on 7.5% polyacrylamide gels, while the sample in *lane 4* was processed on 15% polyacrylamide gel. Molecular weight markers are shown on the side of the blots.

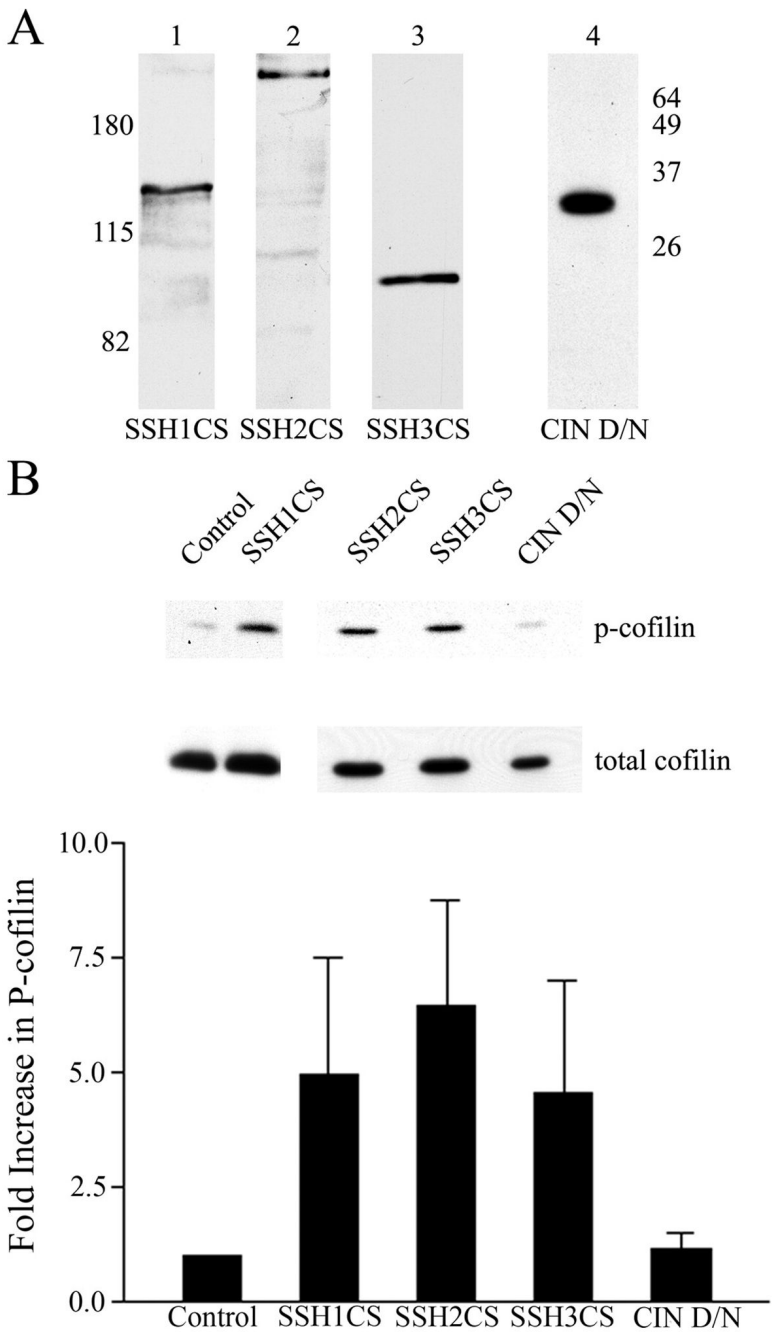

FIGURE 2. Cofilin activity is regulated by SSH proteins and not CIN in human keratinocytes

A, extracts of human keratinocytes infected with adenovirus encoding phosphatase-dead V5-tagged SSH1CS, c-Myc-tagged SSH2CS, V5-tagged SSH3CS, or dominant inactive CIN (*CIN D/N*) were processed for Western immunoblotting and then probed with antibodies that recognize the V5 epitope (*lanes 1* and *3*), the c-Myc epitope (*lane 2*), or with an antibody against CIN (*lane 4*). Samples in *lanes 1–3* were processed on 7.5% polyacrylamide gels, whereas the sample in *lane 4* was processed on 15% polyacrylamide gel. Molecular weight markers are indicated on the sides of the probed blots. *B*, whole cells extracts of uninfected keratinocytes (*Control*) and keratinocytes infected with adenovirus encoding phosphatase-dead SSH1CS, SSH2CS, SSH3CS, or dominant inactive CIN (*CIN D/N*) were processed for

SDS-PAGE/immunoblotting. Blots were probed first with antibodies against phosphorylated cofilin (pSer3) and then with antibodies against total cofilin. The percentage phosphorylation (mean ± S.E. for three independent trials) was calculated relative to total cofilin levels in each of three studies, and the quantification is shown.

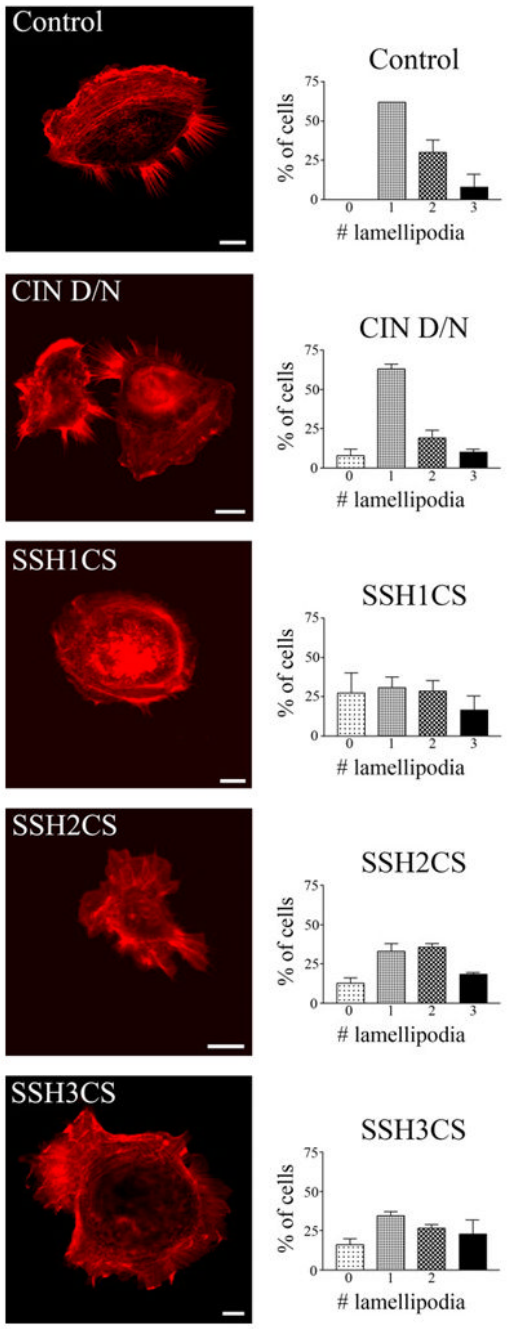

FIGURE 3. Inactivation of SSH proteins changes the organization of the actin cytoskeleton in human keratinocytes

Uninfected human keratinocytes (*Control*) and keratinocytes infected with adenovirus encoding dominant inactive CIN (*CIN D/N*) or phosphatase-dead SSH proteins (*SSH1CS*, *SSH2CS*, and *SSH3CS*) were plated onto glass coverslips, allowed to adhere for 18 –24 h, and then were fixed and stained with rhodamine-phalloidin (*left panels*). The cell preparations were viewed by confocal laser scanning microscopy. In the *right panels*, the number of lamellipodia/cell were counted for each of the cell populations, and the graphs depict the results from 50 cells in each of at least three independent experiments (± S.E.). Representative images are shown in the *left panels. Bars*, 10 μm.

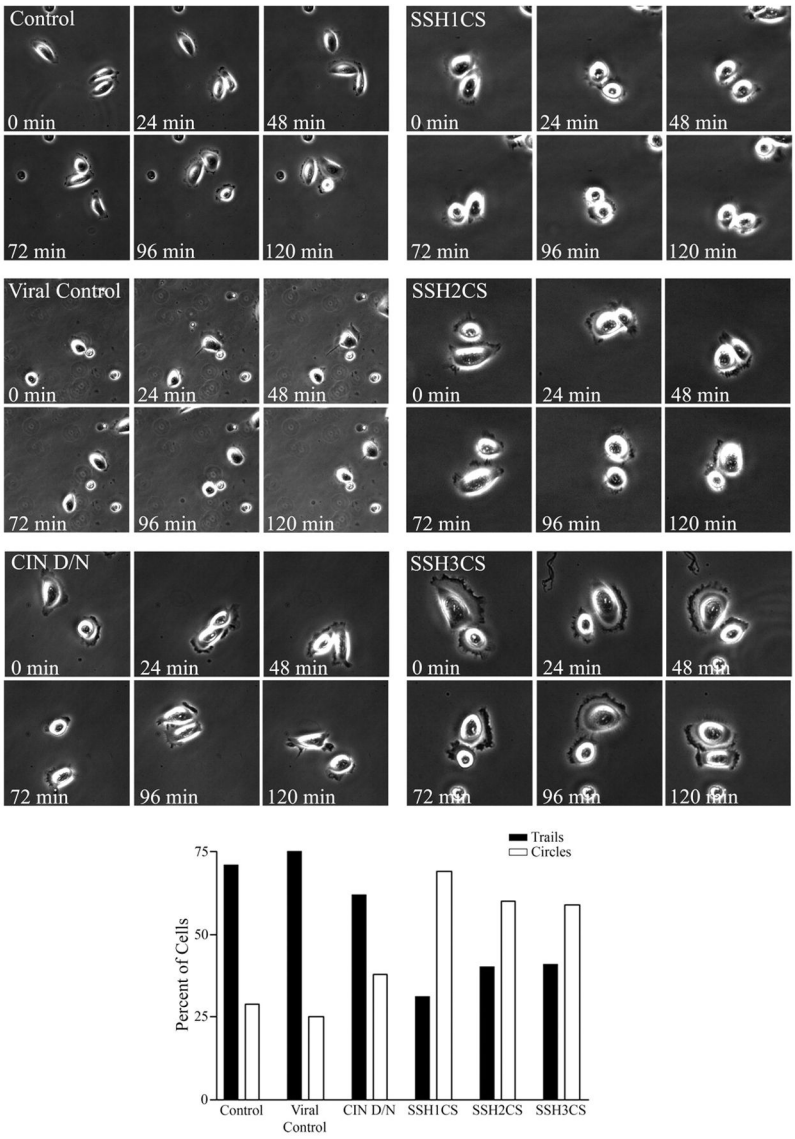

FIGURE 4. Motility assays of keratinocytes on uncoated glass

Human keratinocytes (*Control*) (*n* = 104), keratinocytes infected with control adenovirus (*Viral control*) (*n* = 32), or keratinocytes infected with adenovirus encoding dominant inactive CIN (*CIN D/N*) (*n* = 162), phosphatase-dead SSH1CS (*n* = 201), SSH2CS (*n* = 101), or SSH3CS (*n* = 74) as indicated were replated onto glass-bottomed dishes and allowed to adhere for 18 – 24 h. The cells were then viewed by phase-contrast microscopy with images being captured every 2 min for 2 h. In each panel of six, images at 24-min intervals are presented. The *graph* depicts the percentage of cells exhibiting either migration along trails or motility in circles.

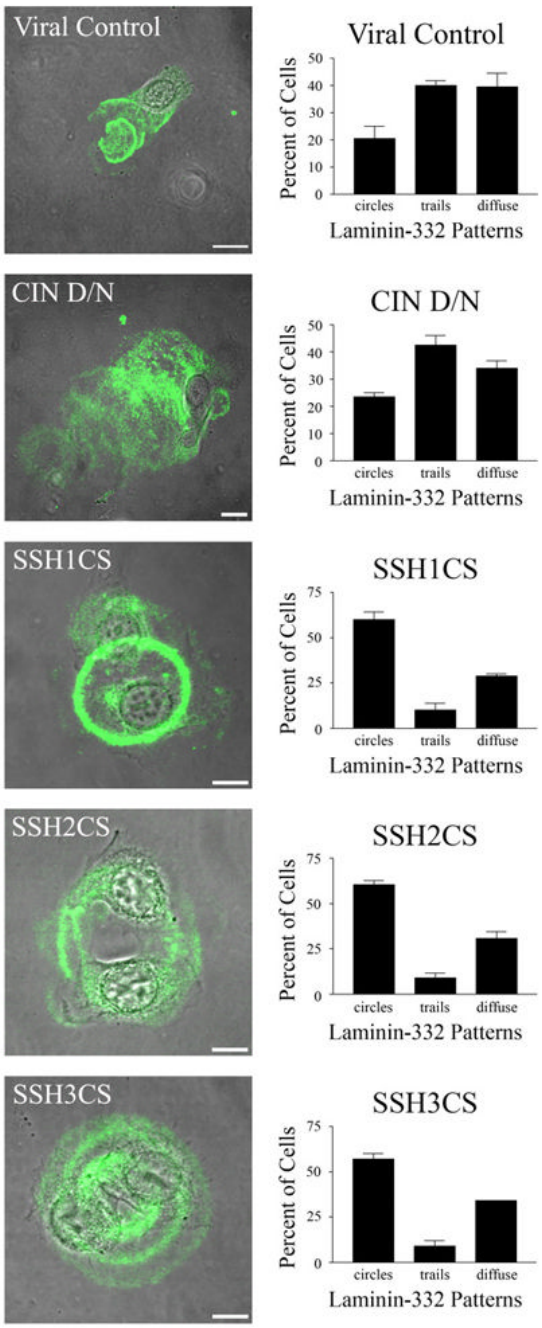

FIGURE 5. Analyses of laminin-332 matrix assembly by keratinocytes

Keratinocytes were infected with control adenovirus (*Viral control*) or adeno-virus encoding dominant inactive CIN D/N, or phosphatase-dead SSH1CS, SSH2CS, or SSH3CS and replated onto glass coverslips 24 h later. At 24 h after plating, cells were prepared for confocal immunofluorescence microscopy using antibody GB3 against the γ2 subunit of laminin-332. *Left panels*, the micrographs show laminin-332 staining patterns overlaid onto the phase-contrast images of the cells. *Right panels*, the percentage of cells displaying laminin-332 patterns in trails, circles, or a diffuse pattern was counted, and the graphs depict analyses of a minimum of 50 cells in each of at least two independent experiments (± S.E.). *Bars*, 20 μm.

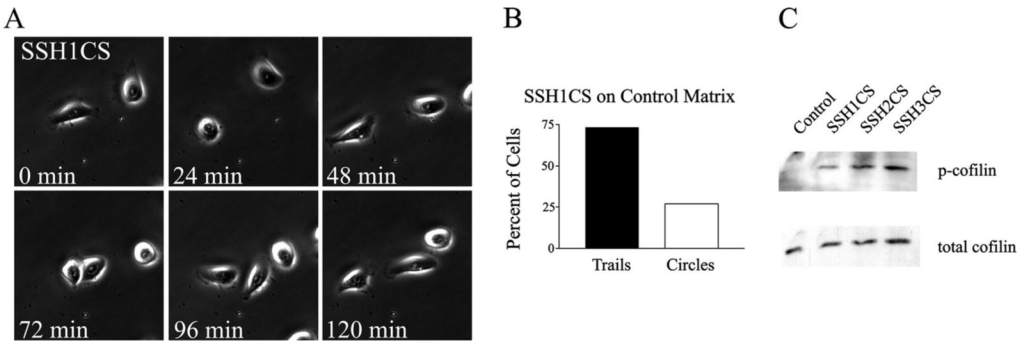

FIGURE 6. Motility assays of keratinocytes expressing phosphatase-dead SSH1CS on preassembled arrays of laminin-332

Keratinocytes were infected with adenovirus encoding SSH1CS, and at 48 h post-infection, the cells were plated onto the laminin-332-rich matrix deposited by uninfected keratinocytes. The cells were allowed to adhere for 2– 4 h, and their motility was analyzed over a period of 2 h. In *panel A*, phase-contrast images of the cells are shown at the indicated time points. *B*, the graph depicts the percentage of cells exhibiting either migration along trails or motility in circles ($n = 41$). *C*, cofilin phosphorylation was measured in whole cell extracts from uninfected keratinocytes or keratinocytes infected with adenovirus encoding SSH1CS, SSH2CS, or SSH3CS that were replated on preformed laminin-332 matrix. Blots were probed first with antibodies against phosphorylated cofilin (pSer3) and then with antibodies against total cofilin.

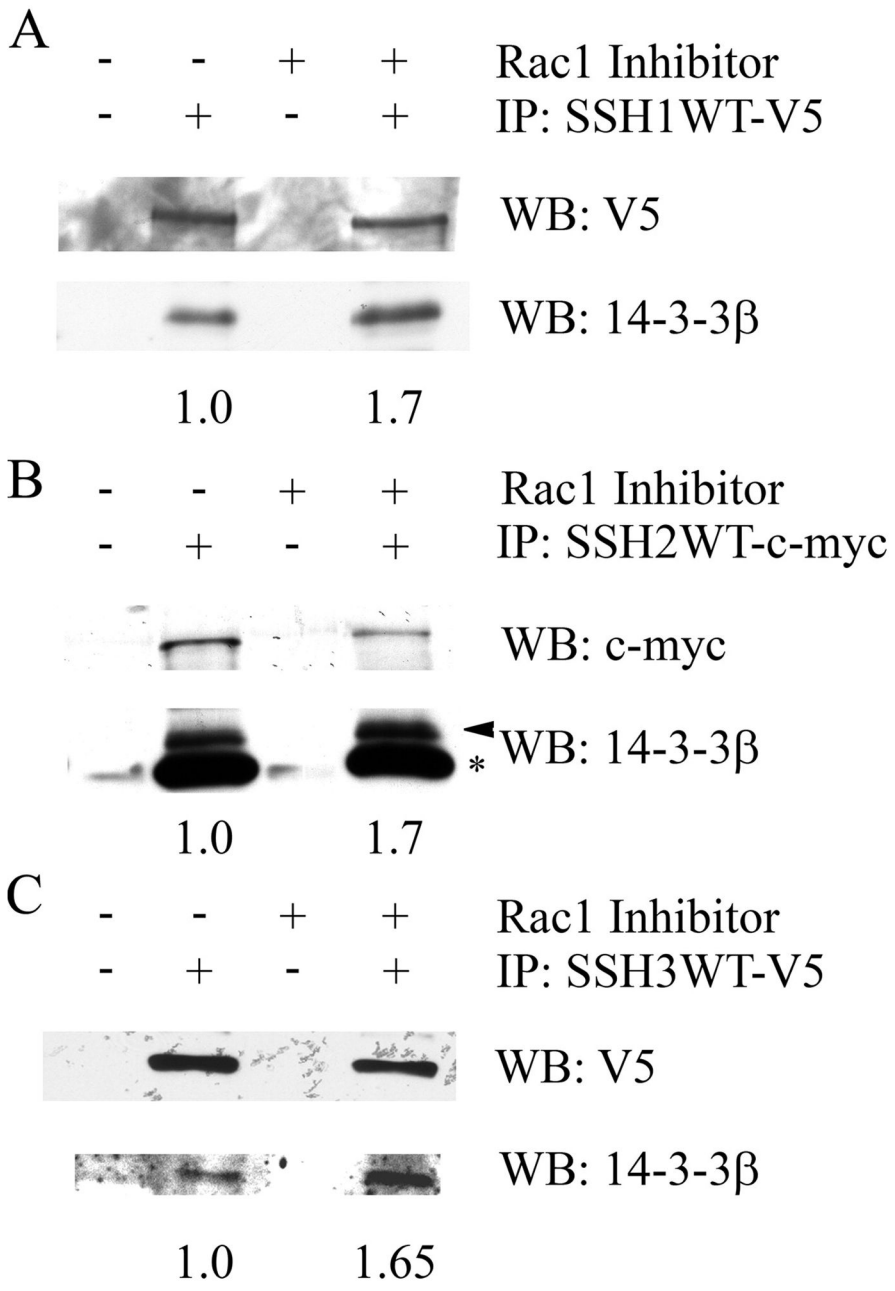

FIGURE 7. Binding of 14-3-3 proteins to SSH proteins in the presence of a Rac1 inhibitor

Extracts of keratinocytes expressing V5-tagged SSH1WT (*A*), c-Myc-tagged SSH2WT (*B*), or V5-tagged SSH3WT (*C*) treated with or without the Rac1 inhibitor NSC23766 were processed for immunoprecipitation using V5 or c-Myc antibodies. A portion of the precipitated proteins was subjected to immunoblotting using a pan-14-3-3 antibody and monoclonal antibodies against V5 or c-Myc as indicated. The levels of SSH proteins that co-precipitate with 14-3-3 proteins from extracts of the Rac1 inhibitor-treated cells relative to non-treated cells, following normalization to either V5- or c-Myc-tagged SSH precipitated proteins, were quantified. These values are indicated under the 14-3-3 blots. *B*, there is a nonspecific reactive species indicated by *. An *arrow* points to the immunoprecipitated 14-3-3 protein in *panel B*.

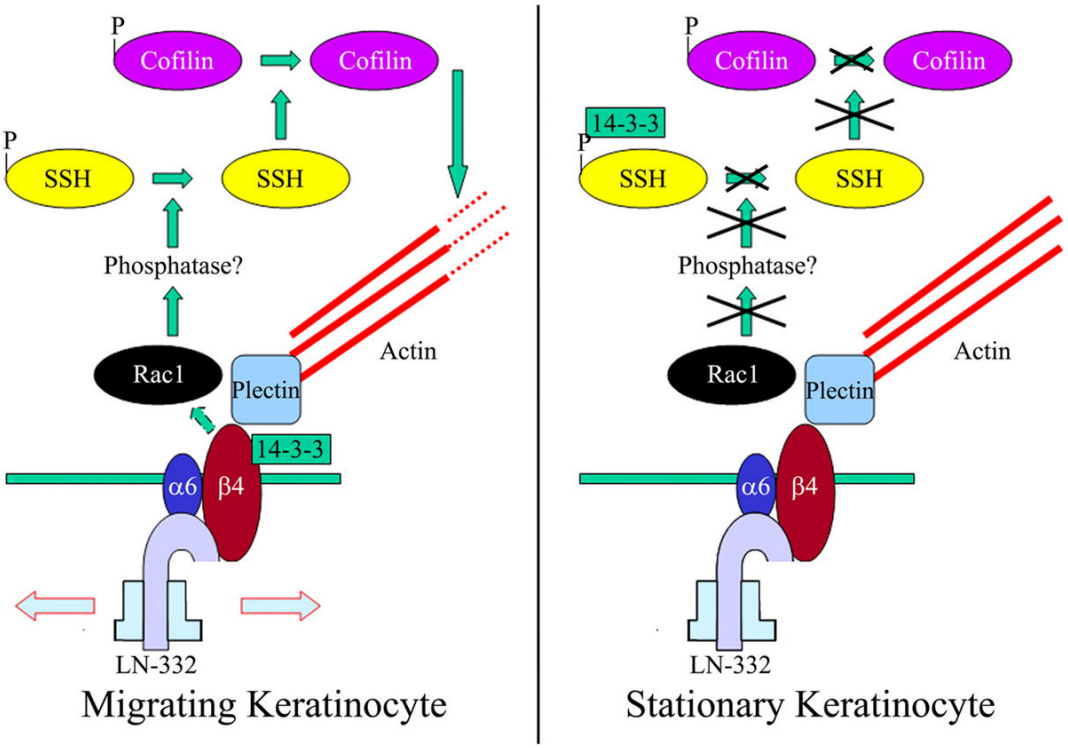

FIGURE 8. This model depicts the putative signaling pathway by which *β*4 integrin regulates the organizational state of laminin-332 in the extracellular matrix in motile *versus* stationary keratinocytes

Our data indicate that it does so through signaling via Rac1, SSH proteins, 14-3-3 proteins, cofilin, and the actin cytoskeleton.